



## Original Article

## Herbal formulation MIT ameliorates high-fat diet-induced non-alcoholic fatty liver disease



Sang-hyun Ahn<sup>a,1</sup>, Eun-Sun Yang<sup>b,1</sup>, Hey-Rin Cho<sup>c</sup>, Syng-Ook Lee<sup>c</sup>, Ki-Tae Ha<sup>b,\*</sup>, Kibong Kim<sup>d,e,\*\*</sup>

<sup>a</sup> Department of Anatomy, College of Korean Medicine, Semyung University, Semyung-ro 65, Jecheon-si, Chungbuk 27136, Republic of Korea

<sup>b</sup> Department of Korean Medical Science, School of Korean Medicine and Korean Medical Research Center for Healthy Aging, Pusan National University, Busandaehak-ro 49, Mulgeum-eup, Yangsan-si, Gyeongsangnam-do 50612, Republic of Korea

<sup>c</sup> Department of Food Science and Technology, Keimyung University, Daegu 42601, Republic of Korea

<sup>d</sup> Second Division of Clinical Medicine, School of Korean Medicine, Pusan National University, Busandaehak-ro 49, Mulgeum-eup, Yangsan-si, Gyeongsangnam-do 50612, Republic of Korea

<sup>e</sup> Department of Korean Pediatrics, Pusan National University Korean Medicine Hospital, Geumo-ro 20, Mulgeum-eup, Yangsan-si, Gyeongsangnam-do 50612, Republic of Korea

## ARTICLE INFO

## Article history:

Received 2 April 2020

Received in revised form 23 April 2020

Accepted 29 April 2020

Available online 14 May 2020

## Keywords:

*Ephedra sinica*

*Panax ginseng*

*Alisma orientale*

Non-alcoholic fatty liver disease

High-fat diet

## ABSTRACT

**Background:** Non-alcoholic fatty liver disease (NAFLD) is one of the most common liver diseases and is caused by obesity, diabetes, high blood pressure, and insulin resistance. Many studies have explored novel candidates to treat NAFLD using herbal medicines owing to their fewer side effects. In this study, we examined the effect of MIT, an herbal formula comprising *Ephedra sinica*, *Panax ginseng*, and *Alisma orientale*, on the murine model of NAFLD.

**Methods:** To evaluate the effect of MIT on NAFLD, we used the high-fat diet (HFD)-induced NAFLD mice model. The mice were divided into four groups: control, HFD, HFD with metformin administration, and HFD with MIT administration. Freeze-dried MIT was dissolved in phosphate buffered saline and orally administered for 8 weeks to MIT-treated mice (60 mg/kg) after feeding them with HFD for 16 weeks.

**Results:** MIT treatment significantly attenuated fat accumulation, serum glucose levels, and excessive cholesterol. It also reduced the activation of NF-κB, JNK, ERK, mammalian target of rapamycin, and peroxisome proliferator-activated receptor γ in the HFD-induced NAFLD mice. The expression level of enzymes involved in the synthesis and oxidation of fatty acids, acetyl-CoA carboxylase and CYP2E1, were clearly reduced by MIT treatment. Reactive oxygen species (ROS) production and subsequent liver damage were effectively reduced by MIT treatment.

**Conclusion:** We suggest that MIT is a potent herbal formula that can be used for the prevention and treatment of obesity-related NAFLD via regulating the levels of serum glucose and free fatty acids, inflammation, lipid accumulation, and ROS-mediated liver damage.

© 2020 Korea Institute of Oriental Medicine. Publishing services by Elsevier B.V. This is an open access article under the CC BY-NC-ND license (<http://creativecommons.org/licenses/by-nc-nd/4.0/>).

## 1. Introduction

Non-alcoholic fatty liver disease (NAFLD) is one of the most important causes of liver disease worldwide, affecting both the

adults and children.<sup>1</sup> A large number of patients with NAFLD progress to the advanced stages of liver diseases, such as non-alcoholic steatohepatitis (NASH) and hepatocellular carcinoma.<sup>2</sup> Although some patients with NAFLD may be lean, the condition is generally regarded as a consequence of obesity and metabolic diseases.<sup>1,3</sup> In addition, obesity, especially from childhood, is a major risk factor for NAFLD-related progression of liver disease.<sup>1,4</sup>

Many researchers have been struggling to develop novel therapies for NAFLD by targeting diverse molecular mechanisms.<sup>5,6</sup> Several candidates, including farnesoid X receptor agonist, peroxisome proliferator-activated receptor (PPAR) agonist, apoptosis signal-regulating kinase-1 inhibitor, and caspase inhibitor are undergoing phase II and phase III clinical trials<sup>5</sup>; however, cur-

\* Corresponding author at: Korean Medical Research Center for Healthy Aging, Pusan National University, Busandaehak-ro 49, Mulgeum-eup, Yangsan-si, Gyeongsangnam-do 50612, Republic of Korea.

\*\* Corresponding author at: Department of Korean Pediatrics, Pusan National University Korean Medicine Hospital, Geumo-ro 20, Mulgeum-eup, Yangsan-si, Gyeongsangnam-do 50612, Republic of Korea.

E-mail addresses: [hagis@pusan.ac.kr](mailto:hagis@pusan.ac.kr) (K.-T. Ha), [kkb@pusan.ac.kr](mailto:kkb@pusan.ac.kr) (K. Kim).

<sup>1</sup> These authors contributed equally in this study.

**Table 1**

The composition of herbal formula, MIT.

Latin name	Part	Korean name	Country origin	Amount
<i>Ephedra sinica</i> Stapf.	Stems and leaves	Mahuang	China	100 g
<i>Panax ginseng</i> C. A. Mayer	Roots	Insam	Korea	100 g
<i>Alisma orientale</i> (Sam.) Juz.	Roots	Taeksa	Korea	100 g
Total				300 g

rently, there are very limited options for the clinical management of NAFLD.<sup>5,7</sup> Diverse herbal medicines and formulas have been studied for the treatment of fatty liver disease, and some herbal medicines have shown a positive effect.<sup>8</sup> Since the past decades, herbal medicines have captured attention as candidate therapeutic agents for the prevention and treatment of NAFLD owing to their high efficacy and low risk of side effects.<sup>9</sup>

MIT, an herbal formula that is composed of the stems and leaves of *Ephedra sinica* Stapf. (Mahuang in Korean), roots of *Panax ginseng* C. A. Mayer (Insam in Korean), and roots of *Alisma orientale* (Sam.) Juz. (Taeksa in Korean). The medicinal herbs have been used to treat obese patients in Korean medicinal clinics.<sup>8</sup> Each herbal ingredients has been reported as an effective therapeutic agent for hyperlipidemia and NAFLD.<sup>10–12</sup> The fermented ginseng or steamed red ginseng is also therapeutically effective in chronic liver diseases, including NAFLD.<sup>13,14</sup> In addition, the extracts of *A. orientale* ameliorated NAFLD or NASH by modulating the oxidative stress, autophagy, and ER stress.<sup>15,16</sup> However, the effects of the combination of these herbal medicines on NAFLD have not been studied previously.

In this study, we examined the effect of MIT on NAFLD using a high-fat diet (HFD)-induced mice model. The results clearly demonstrate that MIT lowered the weight, body fat, and serum levels of glucose via modulating inflammation, lipid accumulation, and reactive oxygen species (ROS)-mediated liver damage. Thus, we suggest that MIT could be a good herbal formula for the prevention and treatment of NAFLD.

## 2. Materials and methods

### 2.1. Preparation of herbal extract of MIT

The medicinal herbs were purchased from Omniherb Co. (Daegu, Korea) and authenticated by the botanical expert in the company. The herbal materials were prepared according to the herbal Good Manufacturing Practice guidelines of Korea Food and Drug Administration (KFDA). The voucher specimens were deposited at the herbarium of the College of Korean Medicine at the Semyung University. Prescription MIT was prepared according to the clinical prescription at the Korean Medical Hospital at the Busan National University as shown in Table 1. The stem and leaves of *E. sinica* (100 g), roots of *P. ginseng* (100 g), and roots of *A. orientale* (100 g) were decocted in 1 L of distilled water at 100 °C for 1 h and then filtered. The decoction was concentrated to 50 ml using a rotary vacuum evaporator and lyophilized to produce 45 g of MIT with 15% yield.

### 2.2. Experimental animals

Six-week-old male C57BL/6 mice were purchased from Orient Bio Inc. (Seongnam, Korea) and bred in a specific pathogen-free animal facility. Mice weighing 20 g were used for this study after acclimatization for 2 weeks prior to the experiments. The experiments were designed to minimize the number of animals used and their suffering. All animal procedures were approved by the Animal Research Ethics Committee of the Semyung Univer-

sity (SMECAE-2017-08-01) and were performed according to the National Institutes of Health guidelines.

### 2.3. Drug administration to mice

The mice were divided into four groups: 1) control, 2) HFD, 3) HFD with metformin administration (Met) and 4) HFD with MIT administration (MIT). Metformin was used as a control drug for treating obesity-related NAFLD.<sup>17</sup> Ten animals in each group were allowed ad libitum access to the HFD (fat, 60%; carbohydrate, 20%; protein, 20%; DIO diet, Research Diet, New Brunswick, NJ) and drinking water for 24 weeks. The freeze-dried MIT was dissolved in phosphate buffered saline (PBS, 100 µl) and orally administered for 8 weeks to the mice in the MIT group (60 mg/kg) after feeding them with the HFD for 16 weeks. To examine the hepatotoxic side effects of MIT, we also administered a high dose of MIT (120 mg/kg) for 8 weeks in addition to the experimental MIT groups (60 mg/kg). For the Met group, we dissolved Met (17 mg/kg, Daewoong Pharmaceutical Co., Seoul, Korea) in PBS and orally administered it for 8 weeks after feeding the mice with the HFD for 16 weeks.

### 2.4. Dual-energy X-ray absorptiometry (DXA) analysis

To examine the distribution of body fat, DXA analysis (Inalyzer; Medikors, Seongnam, Korea) was performed. At the final step of the experiment before scanning, the mice were anesthetized with sodium pentobarbital (50 mg/kg) and were then placed with their stomach down in the DXA machine. After the scan, the fat composition was calculated using the software for DXA analysis.

### 2.5. Blood biochemical analysis

To examine cholesterol and glucose levels, whole blood samples were obtained at the terminal stage of the study by cardiac puncture. Total blood cholesterol was measured using the Cholesterol E kit (BC108-E; YD Diagnostics, Yongin, Korea) after serum separation. Blood glucose levels were measured using the blood glucose monitoring system Freestyle (Therasense Inc. Alameda, CA).

### 2.6. Tissue sample preparation and histochemistry

After sacrificing the mice, the liver tissues were obtained and fixed in 10% neutral buffered formalin at room temperature for 12 h. The fixed liver tissues were embedded in paraffin for serial sectioning at 5-µm thickness. To observe HFD-induced histological changes in fatty liver tissues, we performed Masson's trichrome staining, which is used to detect collagen fiber content and deposition. The tissue sections were fixed in Bouin's fluid at 50 °C to 60 °C for 1 h, and then picric acid was removed with 70% ethanol. The samples were incubated with Weigert's iron hematoxylin for 10 min to stain the nucleus, and then the collagen fibers were stained with Biebrich scalet-acid fuchsin and phosphomolybdic-phosphotungstic acid for 15 min each followed by staining with aniline blue solution for 5 min; the stained samples were then observed under a microscope. To examine the lipids in liver tissue cryosections, the tissues were fixed with 10% formol calcium and were allowed to oxidize for 1 week; subsequently, they were

cryoprotected in 30% sucrose solution. After embedding in Tissue-Plus OCT compound (Thermo Fisher Scientifics, Waltham, MA), 10- $\mu$ m-thick sections were cut on a freezing microtome (Microm International GbmH, Walldorf, Germany). Lipid distribution on the cryosections of the liver tissues was examined after Oil red O staining. The chemicals and reagents that have not been clearly indicated were all purchased from Sigma-Aldrich (St. Louis, MO).

## 2.7. Immunohistochemistry

The liver tissue slices were incubated in proteinase K (20  $\mu$ g/ml) for 5 min for proteolysis and were blocked with 10% normal goat serum for 4 h at room temperature. Then, the samples were incubated for 72 h in a 4°C humidified chamber with the following primary antibodies: mouse anti-PPAR $\gamma$  (1:50, Santa Cruz, CA), mouse anti-p-mTOR (1:50, Santa Cruz, CA), mouse anti-glutathione peroxidase 4 (GPx4) (1:100, Santa Cruz, CA), mouse anti-8-OHdG (1:100, Santa Cruz, CA), mouse anti-caspase 3 (1:100, Santa Cruz, CA), mouse anti-p-IkB (1:250, Santa Cruz, CA), mouse anti-ERK (1:100, Santa Cruz, CA), and mouse anti-p-JNKO (1:100, Santa Cruz, CA). Biotinylated goat anti-mouse IgG (1:100, Abcam, Cambridge, UK) secondary antibodies were incubated for 48 h in a 4°C humidified chamber. Finally, the samples were incubated with the avidin biotin complex solution (ABC kit, Vector Laboratories Inc., Burlingame, CA) for 1 h at room temperature. The immunoreactivity was visualized in a 50-mM Tris-HCl solution (pH 7.4) containing 0.05% 3,3-diaminobenzidine and 0.01% H<sub>2</sub>O<sub>2</sub>, followed by counterstaining with hematoxylin.

## 2.8. Measurement of DPPH radical scavenging activity

The antioxidant activity of MIT was evaluated by the DPPH (1,1-diphenyl-2-picrylhydrazyl) assay.<sup>18</sup> Briefly, 200  $\mu$ l of 0.1-mM DPPH solution (Sigma-Aldrich, St. Louis, MO) was mixed with 100  $\mu$ l cis-5,8,11,14,17-eicosapentaenoic acid (EPA; Sigma-Aldrich, St. Louis, MO) and the MIT extract at various concentrations (0.125–1.0 mg). After incubating for 30 min at room temperature, the transformation to the oxidized (violet) and reduced (yellow) forms of DPPH was measured by recording the decrease in absorbance at 525 nm using a microplate reader (Molecular Devices, San Jose, CA). The DPPH radical scavenging activity was calculated as the ratio of absorbance of sample vs the absorbance of blank after obtaining seven replicates. Ascorbic acid (Sigma-Aldrich, St. Louis, MO) was used as the reference standard.

$$\text{DPPH scavenging activity (\%)} = (1 - \text{absorbance of sample}/\text{absorbance of blank}) \times 100$$

## 2.9. Image analysis and statistical analysis

Any statistically significant difference in the histochemistry and immunohistochemistry data was calculated by image analysis using Image-Pro Plus (Media Cybernetics, Inc., Silver Spring, MD). All data are presented as means  $\pm$  standard errors. Images of randomly selected fields in the liver tissues of each group were acquired at 100 $\times$  magnification, and the images were analyzed with positive pixels/20,000,000 pixels using SPSS software (SPSS 23, SPSS Inc., Chicago, IL). The significance was verified by one-way analysis of variance and post-validation using Tukey's honest significant difference.

## 3. Results

### 3.1. The effect of MIT on the metabolic indices in HFD mice

To identify the efficacy of MIT in HFD-induced murine NAFLD model, we first checked the change in body weight. Total body

weights increased rapidly in all groups in the first 16 weeks but decreased after the administration of MIT and Met for 8 weeks (Fig. 1A). The weight gain in the HFD, Met, and MIT groups was 71%, 69%, and 70%, respectively, after 16 weeks of feeding them with HFD. In the following 8 weeks, the body weight in the HFD group rapidly increased by 102%, whereas the weight gain in the MIT and Met (positive control group) groups was significantly reduced by 50% and 65%, respectively, compared with that in the control group (Fig. 1A).

At this time, we analyzed the mice body fat ratio using DXA. Fig. 1B shows the mice fat composition in the final 24 weeks. The fat mass of HFD group ( $56.4 \pm 0.48\%$ ) was 2.1-fold higher than that of the control group ( $26.8 \pm 0.75\%$ ), whereas the fat content decreased the most in the MIT group ( $42 \pm 0.52\%$ ); the fat content in the Met group was  $50.5 \pm 0.34\%$  (Fig. 1C). Next, we conducted a blood test to examine cholesterol and blood sugar levels. The total cholesterol in the HFD group ( $680 \pm 9 \text{ mg/dl}$ ) was 4.3 times higher than that in the control group ( $160 \pm 4 \text{ mg/dl}$ ), whereas the MIT group ( $360 \pm 8 \text{ mg/dl}$ ) had significantly reduced total cholesterol (by 47%) compared with that in the HFD group (Fig. 1D). This is more effective than the 32% reduction rate observed in the Met group compared with that in the control group ( $463 \pm 6 \text{ mg/dl}$ ). Blood sugar level in the HFD group ( $416 \pm 6 \text{ mg/dl}$ ) was 154% higher than that in the control group ( $164 \pm 4 \text{ mg/dl}$ ), whereas the MIT group ( $261 \pm 4 \text{ mg/dl}$ ) showed a 37% significant decrease compared with that in the HFD group (Fig. 1E). This is also more effective than the 30% reduction rate observed in Met group compared with that observed in the control group ( $291 \pm 5 \text{ mg/dl}$ ). These results indicate that MIT extract is effective in reducing fat.

### 3.2. The effect of MIT on the lipid accumulation in the liver of HFD mice

Obesity due to HFD causes morphological changes in liver tissues. We observed between the central and context of the liver to determine the effect of MIT in NAFLD by histological analysis. The general characteristic features in the HFD group at 24 weeks were the presence of mesh-like cytoplasm filled with numerous lipid vacuoles and macrovesicular steatosis in hepatocytes (Fig. 2A). A lot of these lipid vacuoles were significantly reduced in the MIT group similar to that in the Met positive control group. Regarding the distribution of lipid droplets, assessed by Oil red O staining, hepatocytes containing lipid droplets of various sizes stained dark pink and were observed in the HFD group. However, the MIT group showed light pink staining of hepatocytes containing small lipid droplets. This result was found to be even more pronounced than observed in the Met group. Fig. 2B presents the statistical data from image analysis. The number of lipid vacuoles in hepatocytes in the HFD group were significantly increased by 7-fold compared with that in the control group. However, compared with the HFD group, the MIT group showed a 52% decrease in lipid vacuoles. The Met group showed a decrease in the ratio of lipid vacuoles in the hepatocytes by 37%. Excessive lipid accumulation is accompanied by fatty acid synthesis and oxidation. The acetyl-coA carboxylase (ACC) gene regulates the metabolism of fatty acids, and cytochrome P450 2E1 (CYP2E1) gene is related to basic metabolic reactions, such as fatty acid oxidation. MIT significantly attenuates the expression of CYP2E1 and ACC proteins (Fig. 2A). The immunopositivity of CYP2E1 and ACC, as observed using image analysis, increased in the HFD group, whereas it significantly reduced in the MIT group (Fig. 2C and D). Taken together, the histological analysis demonstrates that MIT is effective in reducing NAFLD.

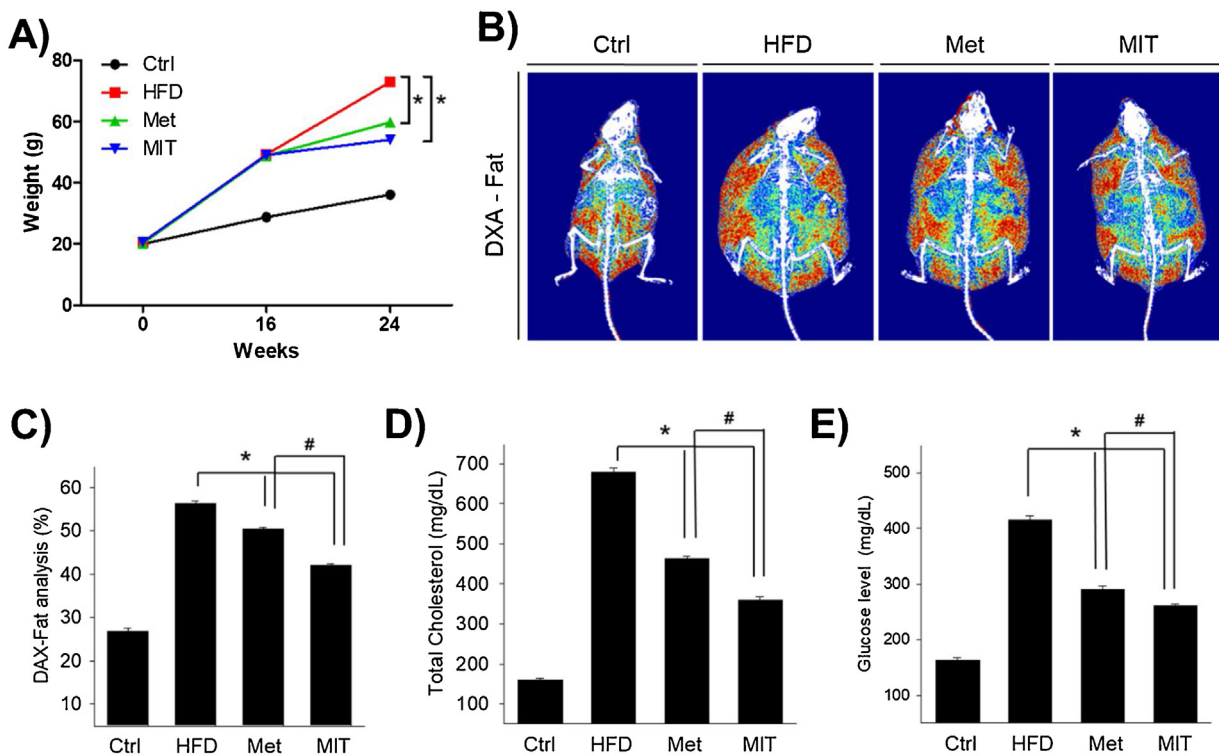


**Fig. 1.** MIT reduces body fat in mice. A) The effects MIT on body weight of HFD-administrated mice was shown. B) DXA images of fat show the alleviation effect of MIT on fat distribution in mice with NAFLD. C) The graph represents DXA image analysis data for the fat distribution in mice. The MIT group had the lowest increase in fat composition. D, E) The mitigating effects of MIT on total cholesterol and glucose levels in mice with NAFLD. Abbreviations: Ctrl, C57BL/6 mice fed with normal diet; DXA, dual-energy X-ray absorptiometry; HFD, C57BL/6 mice fed with high-fat diet; Met, C57BL/6 mice fed with high-fat diet, administered with metformin (17 mg/kg/day) for 8 weeks; MIT, C57BL/6 mice fed with high-fat diet and administered MIT (60 mg/kg/day) extract for 8 weeks; NAFLD, non-alcoholic fatty liver disease. \*, P < 0.05 compared with HFD group; #, P < 0.05 compared with Met group.

### 3.3. The effect of MIT on the activation of NF- $\kappa$ B and mitogen-activated protein kinase (MAPK) signaling pathway

A previous study has showed that HFD can increase NF- $\kappa$ B activation in mice, which leads to IKK level elevation in the liver and adipose tissue.<sup>19</sup> To understand the molecular mechanism underlying MIT activity in attenuating NAFLD, we first examined the changes in NF- $\kappa$ B signaling via immunohistochemistry. In the HFD group, p-I $\kappa$ B was densely observed in the nucleus and cytoplasm around the nuclear membrane in the hepatocytes with lipid accumulation (Fig. 3A). According to the image analysis, p-I $\kappa$ B increased markedly by more than 10-fold in the HFD group than in the control group (Fig. 3B). The MIT group showed a 63% decrease in p-I $\kappa$ B expression than in the HFD group. This is more effective than the 34% reduction ratio of p-I $\kappa$ B in the Met group.

MAPKs also play an important role in the regulation of the metabolism and inflammation, and there are many studies that have investigated the role of MAPKs in liver diseases using genetic animal models.<sup>20</sup> We measured changes in the expression of MAPKs and found that p-ERK was strongly stained in the cytoplasm and p-JNK was strongly stained in the cytoplasm around the nuclear membrane in hepatocytes with lipid accumulation (Fig. 3A). According to the image analysis, p-ERK was significantly increased by more than 15-fold in HFD group than that in the control group (Fig. 3C). However, compared with the HFD group, the Met and MIT groups showed a 37% and 69% decrease, respectively, in p-ERK expression. p-JNK expression was similar to p-ERK expression. p-JNK expression increased markedly by more than 8-fold in the HFD group (Fig. 3D) and decreased by 38% and 55% the Met and MIT groups, respectively, compared with that in the control group. These results show that MIT is effective in relieving HFD-induced NAFLD by suppressing MAPKs and the NF- $\kappa$ B signaling pathway.

### 3.4. The effect of MIT on the mammalian target of rapamycin (mTOR)-PPAR $\gamma$ signaling pathway

The mTOR signaling pathway is a key regulator of obesity, and the signaling axis of mTOR-PPAR $\gamma$  plays an important role in fatty acid uptake, fat accretion, and lipid metabolism in the adipose tissue and liver.<sup>21</sup> To investigate whether the attenuation of NAFLD by MIT is regulated through the mTOR-PPAR $\gamma$  signaling pathway, we performed immunohistochemistry analysis examine the expression and distribution of p-mTOR and PPAR $\gamma$ . Immunolabelling of p-mTOR was observed in the cytoplasm around the nuclear membrane in the hepatocytes with lipid accumulation (Fig. 4A). In the HFD group, the expression of p-mTOR was significantly increased by approximately 18-fold compared with that in the control group (Fig. 4B). However, the expression of p-mTOR in the Met and MIT groups was inhibited by 29% and 47%, respectively. PPAR $\gamma$  immunolabelling was observed in the nucleus and nuclear membrane in hepatocytes with lipid accumulation (Fig. 4A). In the HFD group, the expression of PPAR $\gamma$  was significantly increased by approximately 12-fold compared with that in the control group (Fig. 4C). However, the expression of PPAR $\gamma$  in the Met and MIT groups was inhibited by 26% and 45%, respectively. These results show that the attenuation of NAFLD by MIT is regulated through the modulation of the mTOR- PPAR $\gamma$  signaling pathway.

### 3.5. The effect of MIT on the antioxidant enzyme activity and the ROS-scavenging activity

It is known that oxidative stress is involved in many pathological processes, such as diabetes, obesity, and cardiovascular disease. Fatty acid oxidation is the source of increased mitochondrial ROS production, and upregulation of antioxidant enzymes is

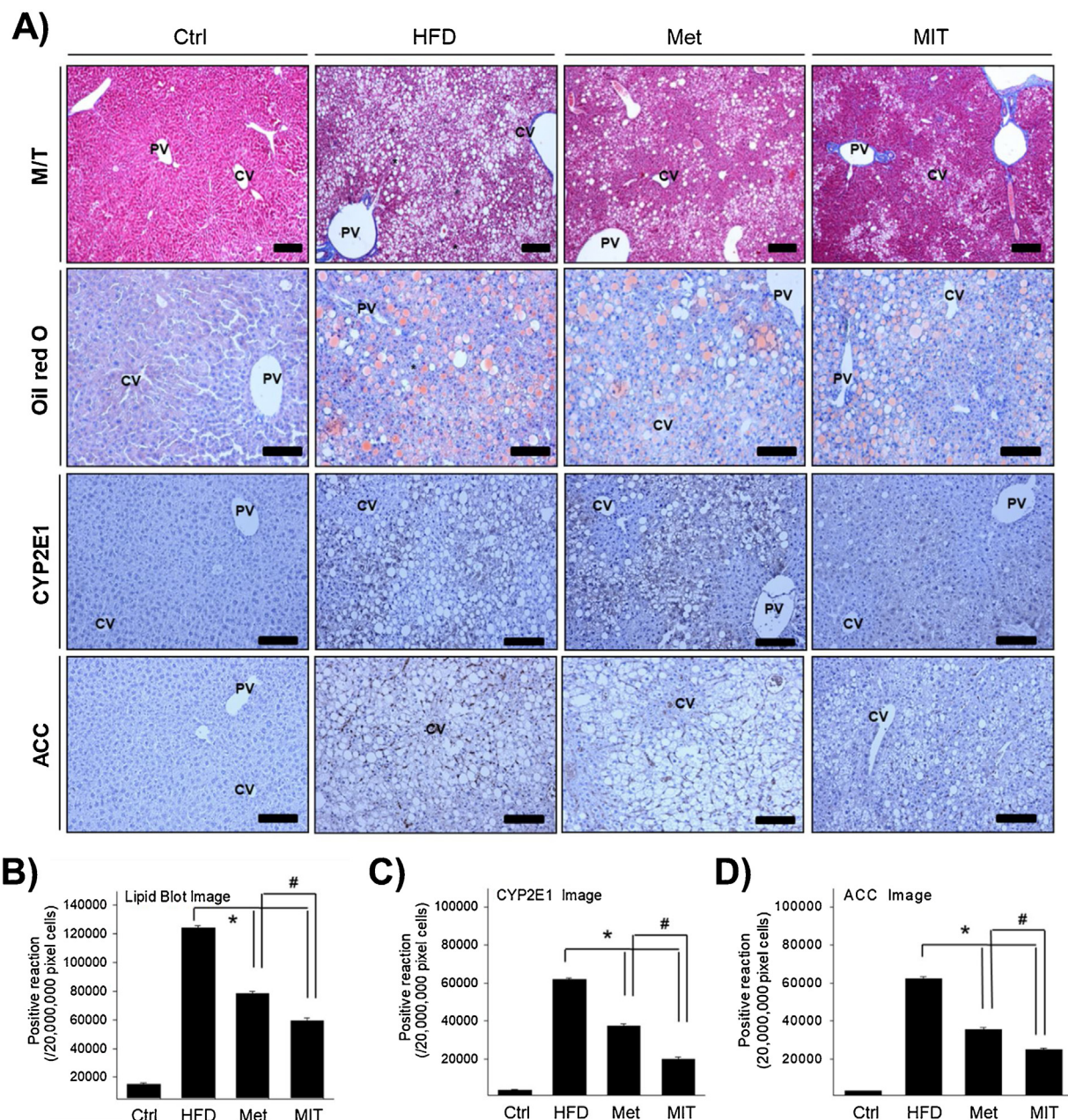


**Fig. 2. Histological analysis of MIT-mediated attenuation of lipid accumulation in the liver of mice with NAFLD.** A) We investigated lipid distribution in the cryosections of liver tissues after Oil red O staining. B) The graph represents the quantification of Oil red O staining shown in panel A. C) Immunohistochemistry shows the expression of CYP2E1 for fatty acid oxidation and ACC for fatty acid synthesis. D-E) The graph represents the number of CYP2E1 and ACC immunopositive cells in each group of figure D. Abbreviations: M/T, Masson trichrome; CV, central vein; PV, portal vein; asterisk, aggregation of hepatocyte with lipid deposition; Ctrl, C57BL/6 mice fed with normal diet; HFD, C57BL/6 mice fed with high-fat diet; Met, C57BL/6 mice fed with high-fat diet, administered with metformin (17 mg/kg/day) for 8 weeks; MIT, C57BL/6 mice fed with high-fat diet and administered MIT (60 mg/kg/day) extract for 8 weeks. \*, P<0.05 compared with HFD group; #, P<0.05 compared with MIT group. Bar size, 50 μm (magnification, 200X).

observed to prevent oxidative damage in diabetes.<sup>22,23</sup> To elucidate the effect of MIT on HFD-induced NAFLD, we measured the expression of GPx4 antioxidant enzyme, which is a glutathione peroxidase that protects the cells against membrane lipid peroxidation. GPx4 immunolabelling was observed in the cytoplasm of hepatocytes with lipid accumulation (Fig. 5A). GPx4 expression in the HFD group was approximately 7-fold greater than that in the control group (Fig. 5B). Interestingly, the expression of GPx4 in the Met and MIT groups increased by 27% and 52%, respectively, compared with that in the HFD group (Fig. 5B). To determine the details, the DPPH radical scavenging activity of the MIT itself was measured. MIT effectively eliminated free radicals in a dose-dependent

manner (Fig. 5C). Together, these observations demonstrate that MIT increased the expression of GPx4 antioxidant enzyme and can remove the free radical in HFD-induced NAFLD.

### 3.6. The effect of MIT on the non-alcoholic liver damage in the liver of HFD mice

ROS produced in HFD-induced NAFLD cause direct or indirect damage to different organs. Excessive oxidative stress can lead to many cellular dysfunctions, such as apoptosis and oxidative damage to DNA, RNA, and proteins, causing strand breaks, protein modifications, and gene mutations. Thus, we confirmed apoptosis

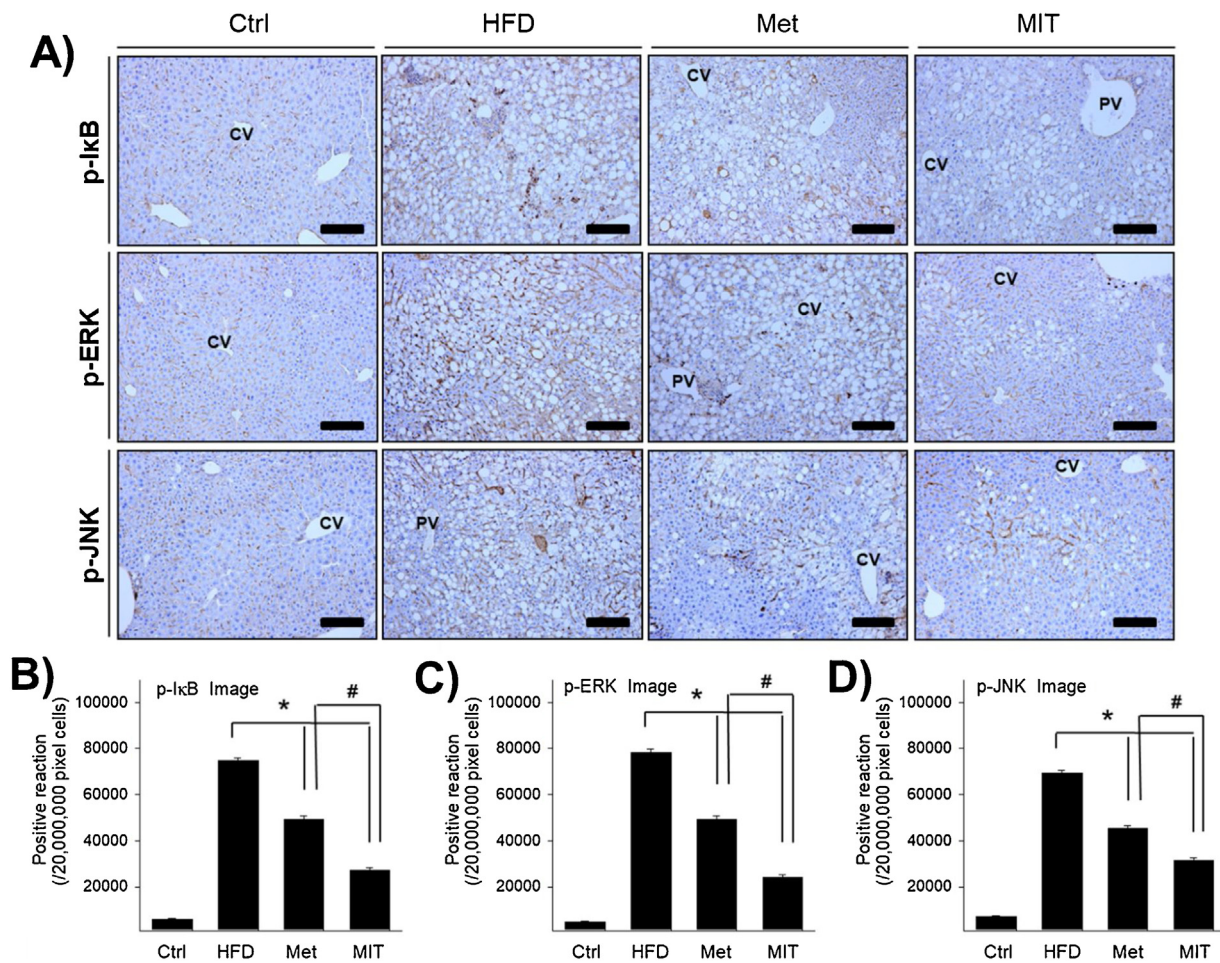


**Fig. 3.** Anti-inflammatory effect of MIT in the liver of mice with NAFLD is associated with the suppression of NF-κB and MAPK signaling pathways. A) Immunohistochemistry shows p-IkB, p-ERK, and p-JNK expression in the liver of mice with NAFLD. B–D) The graph represents the number of p-IkB, p-ERK, and p-JNK immunopositive cells in each group as shown in the images in A). Abbreviations: CV, central vein; PV, portal vein; Ctrl, C57BL/6 mice fed with normal diet; HFD, C57BL/6 mice fed with high-fat diet; Met, C57BL/6 mice fed with high-fat diet and administered metformin (17 mg/kg/day) for 8 weeks; MIT, C57BL/6 mice fed with high-fat diet and administered MIT (60 mg/kg/day) extract for 8 weeks. \**P*<0.05 compared with HFD group; #, *P*<0.05 compared with MIT group. Bar size, 50 μm (magnification, 200X).

induction through caspase-3 immunolabelling and generation of oxidative damage through 8-OHdG immunolabelling, which is one of the most sensitive markers for DNA damage. In immunohistochemistry analysis, 8-OHdG expression was observed in the cytosol of hepatocytes with lipid accumulation (Fig. 6A). The immunoreactivity of 8-OHdG in the HFD group increased by approximately 13-fold compared with that in the control group (Fig. 6B). However, 8-OHdG expression in the Met and MIT groups was decreased by 31% and 95%, respectively, compared with that in the HFD group. Caspase-3 expression also showed a pattern similar to 8-OHdG expression. Caspase-3 immunolabelling was observed in the cytoplasm around the nuclear membrane of hepatocytes with lipid accumulation (Fig. 6A). Caspase-3 expression in the HFD group increased by approximately 18-fold compared with that in the control group (Fig. 6C). However, caspase-3 expression in the Met and MIT groups decreased by 38% and 49%, respectively, compared with that in the HFD group. These results show that oxidative stress by ROS generation in HFD-induced NAFLD can cause DNA damage and cellular apoptosis in the liver, and MIT can effectively attenuate this non-alcoholic liver damage.

#### 4. Discussion

NAFLD is strongly associated with obesity, metabolic syndrome, and insulin resistance, and its incidence is considered to be parallel

to the obesity epidemic.<sup>24,25</sup> In addition, NAFLD can progress from simple fatty liver to an advanced inflammatory stage NASH.<sup>1,5,25</sup> Thus, several genetic, chemical, or dietary animal models have been developed for modeling human NAFLD.<sup>26–28</sup> Unlike other animal models, HFD-induced model mimic both the histopathology and pathogenesis of human NAFLD, as they show the hallmark characteristics of human NAFLD patients, including obesity and insulin resistance.<sup>28</sup> In addition, this model is most widely used and closely resembles obesity-related NAFLD.<sup>5,26</sup> Thus, in this study, we used an HFD-induced mice model.

The mild chronic inflammatory cascades and metabolic signalling pathways are crucial for the progression of NAFLD and NASH.<sup>2,5,29</sup> Chronic metabolic inflammation induced by elevated glucose and free fatty acid mediates the activation of NF-κB, JNK, and ERK signalling pathways in the liver of high-fat fed individuals.<sup>30</sup> In addition, mTOR and PPARγ play key roles in the development and progression of NAFLD through the regulation of metabolic processes, such as fatty acid biosynthesis and oxidation.<sup>31–33</sup>

Accumulated pieces of evidence show that mitochondrial dysfunction is a key player in the progression of NAFLD.<sup>34–36</sup> Mitochondria in the liver of steatotic mice manifests structural and molecular changes.<sup>35,37</sup> This mitochondrial adaptation is linked with mitochondrial ROS formation induced by altered lipid oxidation and antioxidant defenses.<sup>22,35</sup> Glutathione peroxidases, the

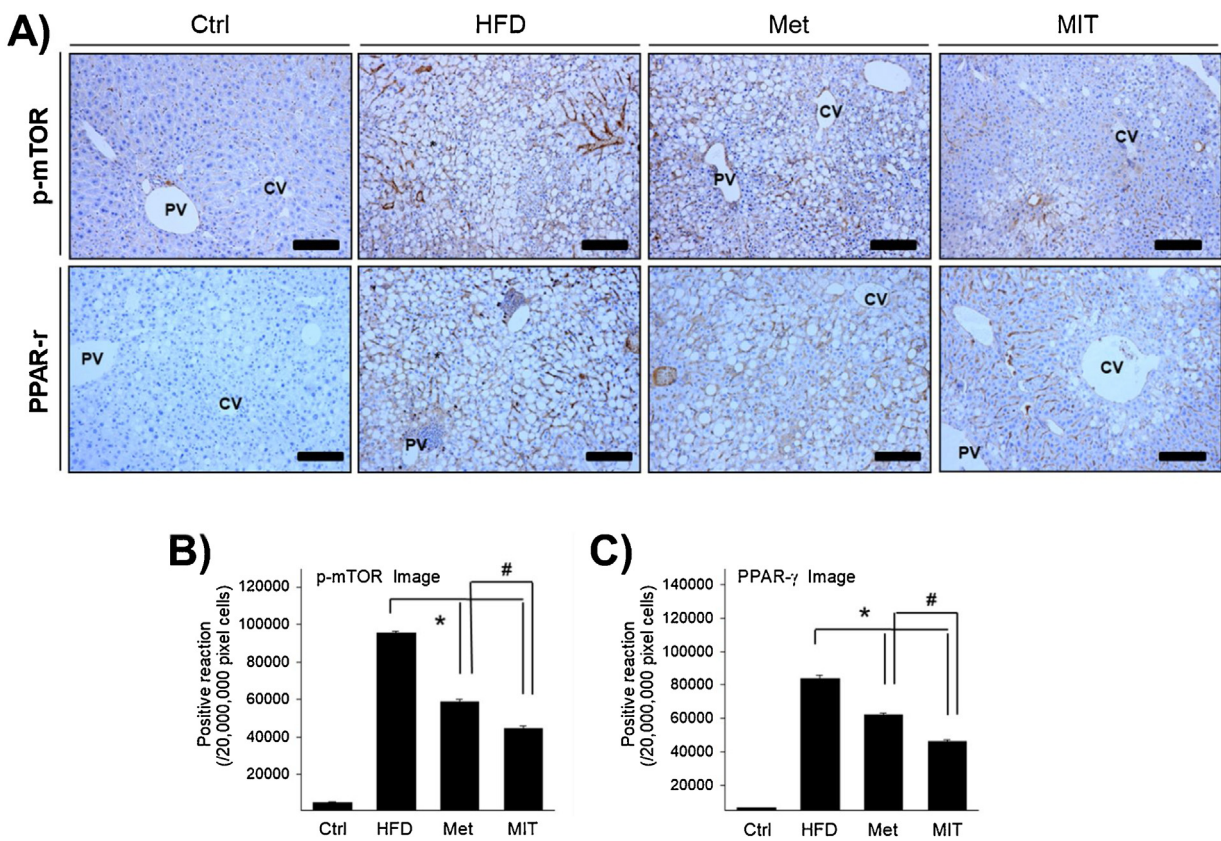


**Fig. 4.** Role of the mTOR signaling pathway in the effect of MIT on NAFLD. A) Immunohistochemistry shows the positive reaction of p-mTOR and PPAR- $\gamma$  in the liver of NAFLD mice. Compared with the HFD group, the MIT group shows attenuated expression of p-mTOR and PPAR- $\gamma$ . B-C) The graph represents the number of p-mTOR and PPAR- $\gamma$  immunopositive cells in each group as shown in A). Abbreviations: CV, central vein; PV, portal vein; Ctrl, C57BL/6 mice fed with normal diet; HFD, C57BL/6 mice fed with high-fat diet; Met, C57BL/6 mice fed with high-fat diet and administered metformin (17 mg/kg/day) for 8 weeks; MIT, C57BL/6 mice fed with high-fat diet and administered MIT (60 mg/kg/day) extract for 8 weeks. \*,  $P < 0.05$  compared with HFD group; #,  $P < 0.05$  compared with MIT group. Bar size, 50  $\mu$ m (magnification, 200X).

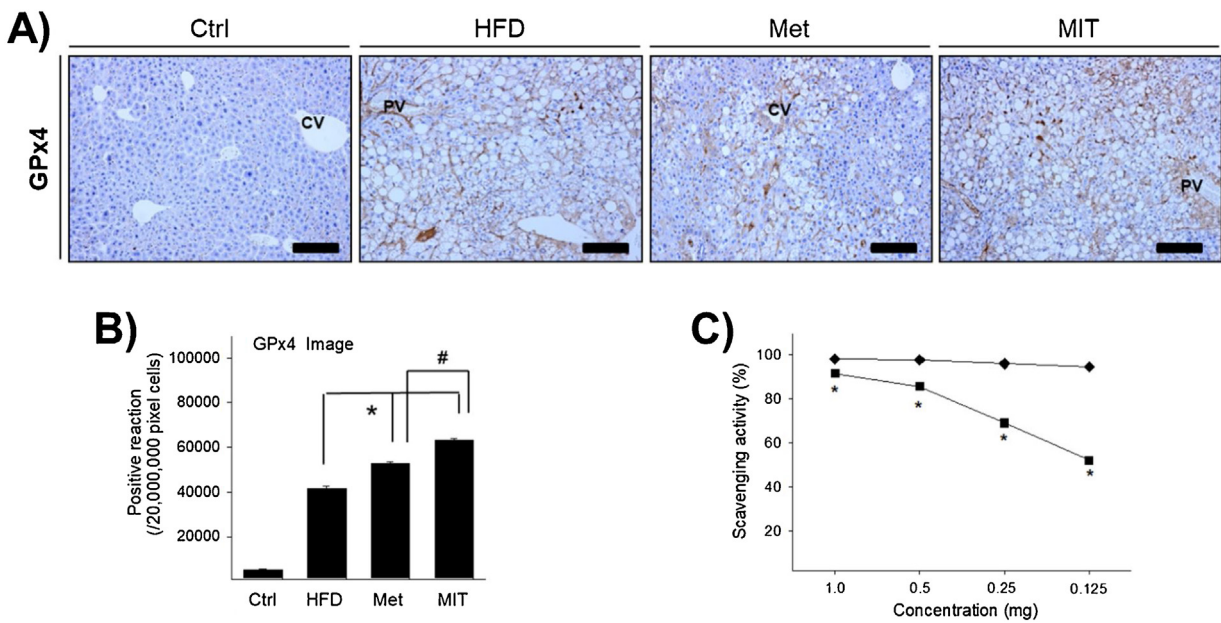


**Fig. 5.** MIT increases the antioxidant enzyme activity and exhibits scavenging activity. A) Immunohistochemistry shows the expression of GPx4 in the liver of NAFLD mice. B) The graph represents the number of GPx4 immunopositive cells as shown in A). C) MIT effectively eliminated the DPPH radical in a dose-dependent manner. Abbreviations: CV, central vein; PV, portal vein; Ctrl, C57BL/6 mice fed with normal diet; HFD, C57BL/6 mice fed with high-fat diet; Met, C57BL/6 mice fed with high-fat diet and administered metformin (17 mg/kg/day) for 8 weeks; MIT, C57BL/6 mice fed with high-fat diet and administered MIT (60 mg/kg/day) extract for 8 weeks. \*,  $P < 0.05$  compared with HFD group; #,  $P < 0.05$  compared with MIT group. Bar size, 50  $\mu$ m (magnification, 200X).

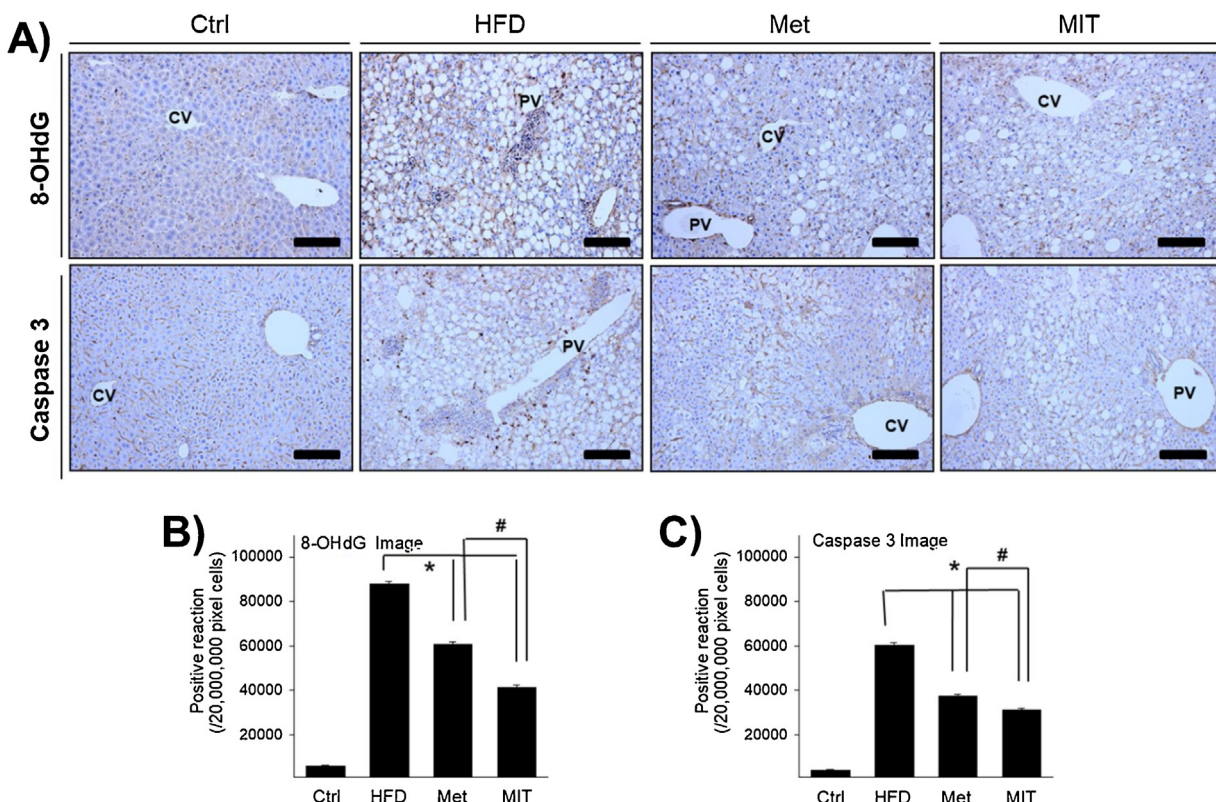


**Fig. 6. MIT decreases non-alcoholic liver damage.** A) Immunohistochemistry shows the expression of 8-OHdG and caspase 3 in the liver of NAFLD mice. B) The graph represents the number of 8-OHdG and caspase 3 immunopositive cells in panel A). Compared with the HFD group, the MIT group shows significantly attenuated non-alcoholic liver damage. Abbreviations: CV, central vein; PV, portal vein; Ctrl, C57BL/6 mice fed with normal diet; HFD, C57BL/6 mice fed with high-fat diet; Met, C57BL/6 mice fed with high-fat diet and administered metformin (17 mg/kg/day) for 8 weeks; MIT, C57BL/6 mice fed with high-fat diet and administered MIT (60 mg/kg/day) extract for 8 weeks. \*, P<0.05 compared with HFD group; #, P<0.05 compared with MIT group. Bar size, 50 μm (magnification, 200X).

enzymes responsible for converting hydrogen peroxide to water via glutathione peroxidation, are the key regulators in the defense of mitochondrial ROS.<sup>38,39</sup> Among them, GPx4 is known as the crucial enzyme for protecting lipid peroxidation in steatotic liver damage by mediating ferroptosis.<sup>40–42</sup> As a consequence of oxidative stress, liver cells frequently undergo oxidative DNA damage and cell death. In NAFLD or advanced fatty liver diseases, 8-OHdG and activated caspase-3 are generally used for detecting DNA damage and activated apoptotic cell death, respectively.<sup>43,44</sup>

In this study, MIT lowered weight gain, serum glucose levels, and excessive cholesterol, which were elevated by HFD. The accumulated fatty acid also diminished by MIT treatment. MIT reduced the expression levels of NF-κB, JNK, ERK, mTOR, and PPARγ, which were increased in the liver of mice in the HFD group. In addition, the representative enzymes involved in the synthesis and oxidation of fatty acids, ACC and CYP2E1,<sup>45,46</sup> respectively, were clearly reduced by MIT treatment. The expression of GPx4 was significantly increased by MIT administration. In addition, the damage to liver cells, measured by 8-OHdG and cleaved form of caspase-3, decreased. Collectively, these data suggest that MIT could be an agent that can prevent the progression of NAFLD to a more advanced type of chronic liver disease, such as NASH, by reducing fat accumulation, ROS production, and subsequent liver damage.

Patients with NAFLD exhibit diverse symptoms, such as fatigue, emotional problems, shortness of breath, diarrhea, swelling of arms and legs, urination problems, and abdominal discomfort.<sup>25</sup> According to the theory of traditional Korean materia medica, the herbal formula, MIT, a combination of *E. sinica*, *P. ginseng*, and *A. orientale*, could be useful in improving physical performance, increasing sympathomimetic energy expenditure, and removing excessive humidity by sweating and urination.<sup>47–49</sup> Thus, we spec-

ulated that these symptoms could be resolved by MIT. Besides traditional theory and clinical effectiveness, the ingredient herbs have been studied as candidates for preventing or treating NAFLD and the diseases related to it, such as obesity and diabetes mellitus.<sup>8–10,15,16,48,50</sup> From these results and previous studies, we suggest that MIT could be a potent candidate herbal formula for treating NAFLD, especially that was related with diabetes mellitus and obesity. To achieve the permission of indication, the evaluation on the efficacy and safety of MIT should be examined by extensive pre-clinical and clinical studies.

The herbal medicine used in this study is generally used in traditional Korean medicine clinics for treating obesity and obesity-related diseases.<sup>9,51,52</sup> The dose for murine administration was calculated according to Nair and Jacob's guideline.<sup>53</sup> The daily dose of 60 mg/kg that was administered to mice is equivalent to 31.92 g/60 kg for humans. The general human use of each ingredient herb is 7.5–15 g/60 kg/day as dried material.<sup>12,47,49</sup> Thus, we suggest that this dose may be recognized as a safe concentration for daily administration in humans. Of the three herbs, only one (*E. sinica*) has been suspected as a hepatotoxic agent at a high dose.<sup>54,55</sup> According to German Commission E, the maximal adult dose for *E. sinica* has been set to 300 mg of total alkaloids,<sup>56</sup> which corresponds to 40 g of dried herb.<sup>57,58</sup> Thus, the dose used in this study is recognized as within the safety limit. In addition, general liver toxicity estimated by histochemical analysis revealed that a 2-fold higher dose of MIT did not show any significant liver toxicity (Fig. S1). However, to precisely examine the safety of MIT, further and extensive toxicity experiments should be performed using good laboratory practices.

In conclusion, we demonstrated that MIT, an herbal formula, combination of three herbal medicines which were used for

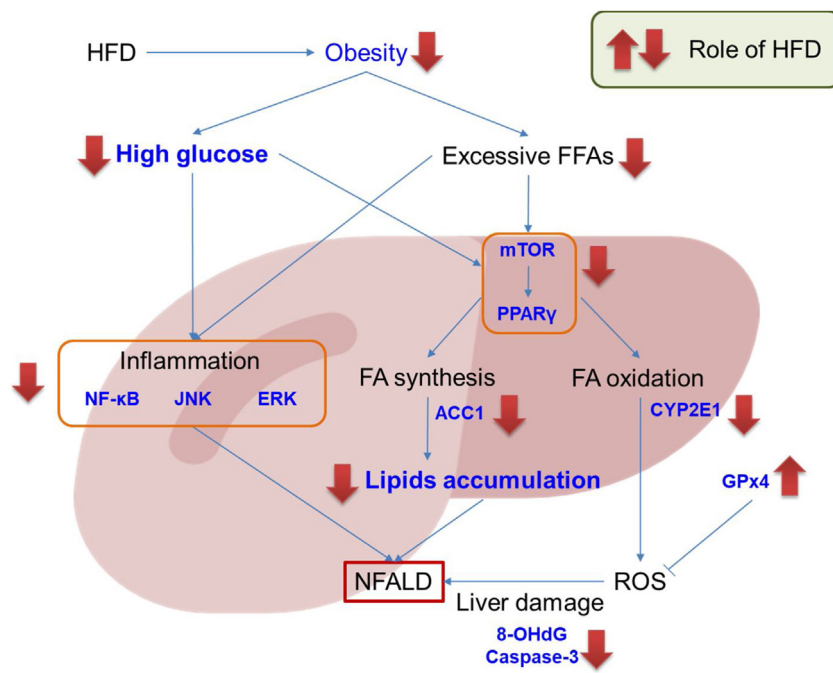


**Fig. 7. Schematic presentation of mode of action of MIT on NAFLD.** MIT has an effect in reducing high-fat diet-induced weight gain and serum glucose and cholesterol levels. MIT can also suppress the NAFLD phenotypes in HFD-fed mice. The mechanisms underlying the suppressive effects of MIT on HFD-induced NAFLD are suggested to involve restriction on inflammation, decrease of lipid accumulation, increment of ROS-defense, and consequent reduction of liver damage.

obesity-related diseases, is effective in reducing weight gain, serum levels of glucose and cholesterol, and NAFLD phenotypes in HFD-fed mice. The possible mechanisms underlying MIT-mediated suppression of NAFLD include restriction on inflammation, a decrease in lipid accumulation, increment in ROS-defense, and consequent reduction in liver damage (Fig. 7). Collectively, these results indicate that MIT could be a novel candidate for the prevention or treatment of obesity-related NAFLD.

### Conflict of interests

The authors have no conflict of interest to declare.

### Funding

This research was supported by the Basic Science Research Program through the National Research Foundation of Korea (NRF) funded by the Ministry of Science and ICT (NRF-2019R1A2C1002443 to K. Kim) and the Ministry of Education (NRF-2019R1F1A105841412 to S. Ahn).

### Author's contribution

SHA performed animal study and immunohistochemistry. ESY supported several experiments. SHA, ESY, HRC, and SOL analyzed the data. ESY, KTH, and KK prepared manuscript. SHA, KTH and KK designed and supervised the study.

### Ethical statement

All animal procedures were approved by the Animal Research Ethics Committee of Semyung University (SMECAE-2017-08-01).

### Data availability

The data will be made available upon request.

### Appendix A. Supplementary data

Supplementary material related to this article can be found, in the online version, at doi:<https://doi.org/10.1016/j.imr.2020.100422>.

### References

- Younossi Z, Anstee QM, Marietti M, et al. Global burden of NAFLD and NASH: trends, predictions, risk factors and prevention. *Nat Rev Gastroenterol Hepatol* 2018;15(1):11–20.
- Michelotti GA, Machado MV, Diehl AM. NAFLD, NASH and liver cancer. *Nat Rev Gastroenterol Hepatol* 2013;10(11):656–65.
- Akhshintala D, Chugh R, Amer F, Cusi K. Nonalcoholic fatty liver disease: the overlooked complication of type 2 diabetes. In: Feingold KR, Anawalt B, Boyce A, et al., editors. *Endotext*. 2000. South Dartmouth (MA).
- Li L, Liu DW, Yan HY, Wang ZY, Zhao SH, Wang B. Obesity is an independent risk factor for non-alcoholic fatty liver disease: evidence from a meta-analysis of 21 cohort studies. *Obes Rev* 2016;17(6):510–9.
- Friedman SL, Neuschwander-Tetri BA, Rinella M, Sanyal AJ. Mechanisms of NAFLD development and therapeutic strategies. *Nat Med* 2018;24(7):908–22.
- Pennisi G, Celsa C, Spatola F, Dallio M, Federico A, Petta S. Pharmacological therapy of non-alcoholic fatty liver disease: what drugs are available now and future perspectives. *Int J Environ Res Public Health* 2019;16(22).
- Bouillet B, Petit J, Sberna A, et al. Application of the new EASL-EASO clinical practice guidelines for the management of non-alcoholic fatty liver disease (NAFLD) in people with type 2 diabetes. *Diabetologia* 2017;60:S573–4.
- Liu ZL, Xie LZ, Zhu J, Li GQ, Grant SJ, Liu JP. Herbal medicines for fatty liver diseases. *Cochrane Database Syst Rev* 2013;(8):CD009059.
- Yao H, Qiao YJ, Zhao YL, et al. Herbal medicines and nonalcoholic fatty liver disease. *World J Gastroenterol* 2016;22(30):6890–905.
- Choi E, Jang E, Lee JH. Pharmacological activities of alisma orientale against nonalcoholic fatty liver disease and metabolic syndrome: literature review. *Evid Based Complement Alternat Med* 2019;2019:2943162.
- Hong M, Lee YH, Kim S, et al. Anti-inflammatory and antifatigue effect of Korean Red Ginseng in patients with nonalcoholic fatty liver disease. *J Ginseng Res* 2016;40(3):203–10.
- Fan Y, Li J, Yin Q, et al. Effect of extractions from Ephedra sinica Stapf on hyperlipidemia in mice. *Exp Ther Med* 2015;9(2):619–25.
- Li Z, Kim HJ, Park MS, Ji GE. Effects of fermented ginseng root and ginseng berry on obesity and lipid metabolism in mice fed a high-fat diet. *J Ginseng Res* 2018;42(3):312–9.
- Park TY, Hong M, Sung H, Kim S, Suk KT. Effect of Korean Red Ginseng in chronic liver disease. *J Ginseng Res* 2017;41(4):450–5.

15. Xu L, Jing M, Yang L, et al. The Alisma and Rhizoma decoction abates nonalcoholic steatohepatitis-associated liver injuries in mice by modulating oxidative stress and autophagy. *BMC Complement Altern Med* 2019;19(1):92.
16. Jang MK, Han YR, Nam JS, et al. Protective effects of alisma orientale extract against hepatic steatosis via inhibition of endoplasmic reticulum stress. *Int J Mol Sci* 2015;16(11):26151–65.
17. Jalali M, Rahimlou M, Mahmoodi M, et al. The effects of metformin administration on liver enzymes and body composition in non-diabetic patients with non-alcoholic fatty liver disease and/or non-alcoholic steatohepatitis: An up-to-date systematic review and meta-analysis of randomized controlled trials. *Pharmacol Res* 2020;104799.
18. Brand-Williams W, Cuvelier ME, Berset C. Use of a free-radical method to evaluate antioxidant activity. *Food Sci Technol-Leb* 1995;28(1):25–30.
19. Dela Pena A, Leclercq I, et al. NF-kappa B activation, rather than TNF, mediates hepatic inflammation in a murine dietary model of steatohepatitis. *Gastroenterology* 2005;129(5):1663–74.
20. Lawan A, Bennett AM. Mitogen-activated protein kinase regulation in hepatic metabolism. *Trends Endocrinol Metab* 2017;28(12):868–78.
21. Wang N, Kong R, Luo H, Xu X, Lu J. Peroxisome proliferator-activated receptors associated with nonalcoholic fatty liver disease. *PPAR Res* 2017;2017:6561701.
22. Rojo AP, Teodoro JS, Palmeira CM. Role of oxidative stress in the pathogenesis of nonalcoholic steatohepatitis. *Free Radic Biol Med* 2012;52(1):59–69.
23. Masarone M, Rosato V, Dallio M, et al. Role of oxidative stress in pathophysiology of nonalcoholic fatty liver disease. *Oxid Med Cell Longev* 2018;2018:9547613.
24. Vernon G, Baranova A, Younossi ZM. Systematic review: the epidemiology and natural history of non-alcoholic fatty liver disease and non-alcoholic steatohepatitis in adults. *Aliment Pharmacol Ther* 2011;34(3):274–85.
25. Houghton-Rahrig LD, Schutte DL, et al. Exploration of symptoms experience in people with obesity-related nonalcoholic fatty liver disease. *Nurs Outlook* 2013;61(4):242–251.e242.
26. Zhong F, Zhou X, Xu J, Gao L. Rodent models of nonalcoholic fatty liver disease. *Digestion* 2019;1:1–14.
27. Castro RE, Diehl AM. Towards a definite mouse model of NAFLD. *J Hepatol* 2018;69(2):272–4.
28. Lau JK, Zhang X, Yu J. Animal models of non-alcoholic fatty liver disease: current perspectives and recent advances. *J Pathol* 2017;241(1):36–44.
29. Blencowe M, Karunayake T, Wier J, Hsu N, Yang X. Network modeling approaches and applications to unravelling non-alcoholic fatty liver disease. *Genes (Basel)* 2019;10(12).
30. Bai L, Li H. Innate immune regulatory networks in hepatic lipid metabolism. *J Mol Med (Berl)* 2019;97(5):593–604.
31. Piccinin E, Villani G, Moschetta A. Metabolic aspects in NAFLD, NASH and hepatocellular carcinoma: the role of PGC1 coactivators. *Nat Rev Gastroenterol Hepatol* 2019;16(3):160–74.
32. Gross B, Pawlak M, Lefebvre P, Staels B. PPARs in obesity-induced T2DM, dyslipidaemia and NAFLD. *Nat Rev Endocrinol* 2017;13(1):36–49.
33. Bakan I, Laplante M. Connecting mTORC1 signaling to SREBP-1 activation. *Curr Opin Lipidol* 2012;23(3):226–34.
34. Simoes ICM, Fontes A, Pinton P, Zischka H, Wieckowski MR. Mitochondria in non-alcoholic fatty liver disease. *Int J Biochem Cell Biol* 2018;95:93–9.
35. Sunny NE, Bril F, Cusi K. Mitochondrial adaptation in nonalcoholic fatty liver disease: novel mechanisms and treatment strategies. *Trends Endocrinol Metab* 2017;28(4):250–60.
36. Wang Y, Palmfeldt J, Gregersen N, et al. Mitochondrial fatty acid oxidation and the electron transport chain comprise a multifunctional mitochondrial protein complex. *J Biol Chem* 2019;294(33):12380–91.
37. Einer C, Hohenester S, Wimmer R, et al. Mitochondrial adaptation in steatotic mice. *Mitochondrion* 2018;40:1–12.
38. Lucena MI, Garcia-Martin E, Andrade RJ, et al. Mitochondrial superoxide dismutase and glutathione peroxidase in idiosyncratic drug-induced liver injury. *Hepatology* 2010;52(1):303–12.
39. Booty LM, Gawel JM, Cvetko F, et al. Selective disruption of mitochondrial thiol redox state in cells and in vivo. *Cell Chem Biol* 2019;26(3):449–461.e448.
40. Qi J, Kim JW, Zhou Z, Lim CW, Kim B. Ferroptosis affects the progression of nonalcoholic steatohepatitis via the modulation of lipid peroxidation-mediated cell death in mice. *Am J Pathol* 2019.
41. Cozza G, Rossetto M, Bosello-Travaini V, et al. Glutathione peroxidase 4-catalyzed reduction of lipid hydroperoxides in membranes: The polar head of membrane phospholipids binds the enzyme and addresses the fatty acid hydroperoxide group toward the redox center. *Free Radic Biol Med* 2017;112:1–11.
42. Garcia-Berumen CI, Ortiz-Avila O, Vargas-Vargas MA, et al. The severity of rat liver injury by fructose and high fat depends on the degree of respiratory dysfunction and oxidative stress induced in mitochondria. *Lipids Health Dis* 2019;18(1):78.
43. Seki S, Kitada T, Yamada T, Sakaguchi H, Nakatani K, Wakasa K. In situ detection of lipid peroxidation and oxidative DNA damage in non-alcoholic fatty liver diseases. *J Hepatol* 2002;37(1):56–62.
44. Akazawa Y, Nakao K. To die or not to die: death signaling in nonalcoholic fatty liver disease. *J Gastroenterol* 2018;53(8):893–906.
45. Kim CW, Addy C, Kusunoki J, et al. Acetyl CoA carboxylase inhibition reduces hepatic steatosis but elevates plasma triglycerides in mice and humans: a bedside to bench investigation. *Cell Metab* 2017;26(3):576.
46. Kohjima M, Enjoji M, Higuchi N, et al. Re-evaluation of fatty acid metabolism-related gene expression in nonalcoholic fatty liver disease. *Int J Mol Med* 2007;20(3):351–8.
47. Tian T, Chen H, Zhao YY. Traditional uses, phytochemistry, pharmacology, toxicology and quality control of Alisma orientale (Sam.) Juzep: a review. *J Ethnopharmacol* 2014;158(Pt A):373–87.
48. Kim BS, Song MY, Kim H. The anti-obesity effect of Ephedra sinica through modulation of gut microbiota in obese Korean women. *J Ethnopharmacol* 2014;152(3):532–9.
49. Choi J, Kim TH, Choi TY, Lee MS. Ginseng for health care: a systematic review of randomized controlled trials in Korean literature. *PLoS One* 2013;8(4):e59978.
50. Song MK, Um JY, Jang HJ, Lee BC. Beneficial effect of dietary Ephedra sinica on obesity and glucose intolerance in high-fat diet-fed mice. *Exp Ther Med* 2012;3(4):707–12.
51. Liu Y, Sun M, Yao H, Liu Y, Gao R. Herbal medicine for the treatment of obesity: an overview of scientific evidence from 2007 to 2017. *Evid Based Complement Alternat Med* 2017;2017:8943059.
52. Wang J, Feng B, Xiong X. Chinese herbal medicine for the treatment of obesity-related hypertension. *Evid Based Complement Alternat Med* 2013;2013:757540.
53. Nair AB, Jacob S. A simple practice guide for dose conversion between animals and human. *J Basic Clin Pharm* 2016;7(2):27–31.
54. Nadir A, Agrawal S, King PD, Marshall JB. Acute hepatitis associated with the use of a Chinese herbal product, ma-huang. *Am J Gastroenterol* 1996;91(7):1436–8.
55. Neff GW, Reddy KR, Durazo FA, Meyer D, Marrero R, Kaplowitz N. Severe hepatotoxicity associated with the use of weight loss diet supplements containing ma huang or usnic acid. *J Hepatol* 2004;41(6):1062–4.
56. Blumenthal M, Brinckmann J, Wollschlaeger B. *The ABC clinical guide to herbs*. 1st ed. Austin, Tex.: American Botanical Council; 2003.
57. Liu YM, Sheu SJ. Determination of ephedrine alkaloids by capillary electrophoresis. *J Chromatogr* 1992;600(2):370–2.
58. Liu YM, Sheu SJ, Chiou SH, Chang HC, Chen YP. A comparative-study on commercial samples of Ephedrae-Herba. *Planta Med* 1993;59(4):376–8.